Hindawi
Complexity
Volume 2024, Article ID 5316162, 16 pages
https://doi.org/10.1155/2024/5316162

Research Article

Ripple-Spreading Network of China's Systemic Financial Risk Contagion: New Evidence from the Regime-Switching Model

Beibei Zhang,[1] Xuemei Xie ,[1] and Xi Zhou[2]

[1]*School of Economics and Management, Beijing University of Posts and Telecommunications, Beijing 100876, China*
[2]*Jiyang College of Zhejiang A&F University, Shaoxing 311800, China*

Correspondence should be addressed to Xuemei Xie; xxuem@bupt.edu.cn

Received 10 October 2023; Revised 8 January 2024; Accepted 14 February 2024; Published 4 March 2024

Academic Editor: Hiroki Sayama

A better understanding of financial contagion and systemically important financial institutions (SIFIs) is essential for the prevention and control of systemic financial risk. Considering the ripple effect of financial contagion, we integrate the relevant spatiotemporal information that affects financial contagion and propose to use the ripple-spreading network to simulate the dynamic process of risk contagion in China's financial system. In addition, we introduce the smooth-transition vector autoregression (STVAR) model to identify "high" and "low" systemic risk regimes and set the relevant parameters of the ripple-spreading network on this basis. The results show that risk ripples spread much faster in high than in low systemic risk regimes. However, systemic shocks can also trigger large-scale risk contagion in the financial system even in a low systemic risk regime as the risk ripple continues. In addition, whether the financial system is in a high or low systemic risk regime, the risk ripples from a contagion source (i.e., a real estate company) spread first to the real estate sector and the banking sector. The network centrality results of the heterogeneous ripple-spreading network indicate that most securities and banks and some real estate companies have the highest systemic importance, followed by the insurance, and finally the diversified financial institutions. Our study provides a new perspective on the regulatory practice of systemic financial risk and reminds regulators to focus not only on large institutions but also on institutions with strong ripple capacity.

1. Introduction

Financial security is an important part of national security; preventing and defusing financial risk, especially holding the bottom line of no systemic financial risk, is of great significance to ensure the smooth operation of China's economy and finance. In recent years, many financial institutions in China have been engaged actively in cross-financial business and conduct mixed financial services [1], which have strengthened the linkages between financial institutions and increased systemic risk [2]. Besides, the events of 2008 global financial crisis have reminded us that regulating financial institutions or markets in isolation and ignoring the connectedness between institutions or markets can no longer effectively prevent and control systemic financial risk [3]. Therefore, it is essential and urgent to explore the connectedness among financial institutions in China and examine the spillover and contagion effects of systemic risk by considering the financial system as a whole.

The global financial crisis in 2008 has aroused attention to the connectedness and risk contagion among financial institutions or markets and increased the emergence of related research methods. A commonly used measure of systemic financial risk is the conditional value-at-risk (CoVaR) and the delta conditional value-at-risk (ΔCoVaR) [4], which are based on a "bottom-up" perspective and reflect the risk contribution of financial institutions to the system [5–7]. Another commonly used measure is the marginal expected shortfall (MES) [3], which is based on an "up-bottom" perspective and focuses on the systemic risk contribution of individual financial institution when the system is in a crisis [8]. In addition, the conditional expected shortfall (CoES) [9, 10] and the SRISK risk index [11, 12], etc., have also been developed to measure systemic financial risk. Although methods such as CoVaR, MES, CoES, and SRISK are widely used, they ignore the connectedness in the financial system and take less account of the risk contagion effect. While the contagion effect of risks is at the heart of the outbreak of the systemic risk or financial crisis, when individual or local risk emerges, different institutions may be affected by risk sharing, risk spreading, and risk amplification mechanisms, resulting in chain reactions and even the collapse of the entire financial system.

Network theory, another important branch of systemic risk research, provides an effective and intuitive analytical tool for systemic financial risk by constructing network nodes and edges, which can not only display the risk contagion paths but also identify systemically important nodes [13], and thus helps the regulators to establish a stable financial system and an effective regulatory system. In general, there are two types of financial network analysis methods. The first method uses detailed information on interbank asset-liability exposures to construct financial networks and then determines the specific risk transmission mechanisms or simulates the impact of shocks on the network. Based on this method, scholars have established the interbank exposure network [14], interbank payment network [15, 16], and asset-liability network [17, 18]. Although this method allows for the identification of specific directions and paths of risk contagion, it relies on nonpublic data, which makes research limited. The second method uses financial market data, i.e., stock prices (e.g., return, volatility, and tail risk) to build financial networks and then assesses risk contagion through network topology indicators. Since financial market data are publicly available and forward-looking, they are widely used in the study of financial networks and systemic risk. Related studies mainly include correlation-based networks [19–21], Granger causality networks [22–24], volatility spillover networks [25–27], and tail risk spillover networks [28, 29]. In addition, in order to take more risk information into account, some scholars have developed composite networks [30] and multilayer information spillover networks [31–34]. In these financial networks, nodes denote financial institutions or markets, and edges denote relationships between nodes. By examining whether there are correlation, causality, or spillover effects between nodes, we can determine the risk contagion paths.

In summary, the research on systemic risk under financial network has yielded rich results. It is worth noting that, however, most of the relevant network analyses are static. Although relevant studies have used the rolling time window approach [27, 30, 34] to capture the dynamics of risk contagion, they are unable to model the dynamic ripple effects triggered by a contagion source, i.e., which financial institution is affected first and which is affected later when a financial institution suffers a loss or goes bankrupt. The ripple effect describes the gradual spreading of the effects caused by local events. In fact, the formation and evolution of many real-world complex systems depend to a large extent on the spreading of a few local events [35]. Suppose a failed (lost or bankrupt) financial institution triggers financial contagion, the contagion will spread around like ripples in a calm pond. When it reaches the nearest (highest associated) financial institution, the institution may be infected and trigger a new ripple-spreading process, which is analogous to a ripple in a pond reaching a stake and creating a new responding ripple due to the reflection effect. As the contagion continues to spread, more and more institutions may be infected. It is well known that many successful artificial intelligence (AI) techniques are actually inspired by certain natural system or phenomena [36, 37]. For example, genetic algorithms (GA) are inspired by the process of natural selection and evolution, particle swarm optimization (PSO) is inspired by the learning behaviors within populations, and artificial neural networks (ANNs) are inspired by animal brains, etc. These algorithms or their derived algorithms are also widely used in economic and financial fields [38, 39]. Following the common practice of learning from nature in the field of artificial intelligence, Hu et al. [35] developed a ripple-spreading network model (RSNM) which is inspired by the natural ripple-spreading phenomenon on the calm water surface and emphasized its application potential and flexibility in their paper. On this basis, Hu et al. [40] attempted to apply the genetic algorithm (GA) to tune the ripple-spreading related parameters and made it a great flexibility to study many real-world complex network systems.

Existing studies have shown that financial contagion has ripple effects [41]. Looking at the latest research, several scholars have applied the ripple-spreading network to model the contagion path of financial risk and identify systemically important financial institutions or markets. For example, Su et al. [42] proposed a ripple network-based collective spillover effect approach and identified the systemic importance of financial markets. Xu et al. [43] pointed out that the ripple effect is one of the most features of financial contagion and modeled the paths of China's systemic risk contagion under different contagion sources. However, the results are far from sufficient, and there are still some issues that need to be further explored. For example, few literature studies have analyzed the ripple effect of financial contagion in the framework of regime switching. Financial markets may experience regime shifts and nonlinear risk contagion as a result of sudden structural changes due to selling behavior of common asset holders [44], investor panic [45], and asymmetric dependence on financial asset returns in both upward and downward phases of the market [46]. Feng et al. [47] pointed out that macroeconomic and financial variables often have sudden structural changes due to the exposure to external shocks such as policy changes and ignored the possible effects of regime shifts in the process of risk contagion which may lead to a significant bias. Therefore, it is necessary and urgent to explore the network connectedness and examine the dynamic ripple-spreading process of financial risk under different systemic risk regimes. In addition, relevant studies have examined financial contagion in the framework of a deterministic ripple-spreading network. However, the deterministic and uncertain factors coexist in the process of financial contagion, and how to balance this relationship deserves further exploration. In this paper, we mainly carry out the following innovative work.

First, we improve the basic algorithm of the ripple-spreading network to make it applicable to financial contagion and apply it to the analysis of financial contagion in China. The semideterministic ripple-spreading network model (SD-RSNM) can balance the deterministic and uncertain factors in the process of financial contagion. By observing the instantaneous state of the ripple-spreading network, we can identify which financial institutions are affected first and which are affected later.

Second, we introduce the smooth-transition vector autoregression (STVAR) model to identify the "high" and "low" state regimes of systemic risk and parameterize the ripple-spreading network on this basis. In terms of parameter specification, we take into account some important spatiotemporal factors affecting financial contagion, such as the magnitude of financial shock, risk amplification factor, risk resistance ability, and spreading speed of each financial institution.

Finally, we manage to identify systemically important financial institutions (SIFIs) based on the heterogeneous networks generated by the dynamic ripple-spreading processes under high and low systemic risk regimes. We find that most securities and banks and some real estate companies have the highest systemic importance in China's financial system. In particular, the securities sector has the strongest ripple-spreading capacity and plays an intermediary role in the system network. The results remind financial regulators and government departments that systemic risk regulation should focus not only on large institutions but also on institutions with strong ripple effects.

The remainder of the article is structured as follows: Sections 2 and 3 describe the methodology and data, respectively. In Section 4, we apply our method to Chinese financial institutions and present the empirical analysis results. In Section 4, we provide a brief discussion of the findings.

2. Methodology

2.1. Basic Idea of the Ripple-Spreading Network. Considering the simultaneous existence of deterministic and uncertain factors in financial contagion, we derive the semi-deterministic ripple-spreading network model (SD-RSNM) based on Hu et al. [35] and Xu et al. [43] to simulate financial contagion in China's financial system. In this model, there are two classes of parameters: contagion source related and network node related. The parameters of the contagion source include E_0, s_0, and d_{0i}. E_0 denotes the energy of the initial ripple of the contagion source, and it measures the magnitude of the systemic shock; s_0 denotes the ripple-spreading speed of the contagion source; d_{0i} denotes the distance between the contagion source and node i. The parameters of the network nodes include α_i, β_i, s_i, and d_{ij} $(i, j = 1, 2, \cdots, N)$. α_i denotes the risk amplifying factor of the node i; β_i denotes the connection threshold, representing the risk resistance capability of the node i; d_{ij} is the distance between the node i and j. Once a node is infected, it will trigger a new ripple with energy E_i and speed s_i. In addition, the energy parameters, i.e., E_0 and E_i, decay following the same function $f_{\mathrm{Decay}}(E_i, r(i,t)) = \eta E_i/2\pi r(i,t)$, where η is a constant and $r(i,t)$ is the ripple radius of the node i at time t. It is worth noting that, in the framework of SD-RSNM, the node j follows the following activation principles: if $d_{\mathrm{ij}} \leq r(i,t)$ and $f_{\mathrm{Decay}}(E_i, r(i,t)) \geq \beta_j$, then the node j is activated by the node i, while if $d_{\mathrm{ij}} \leq r(i,t)$ and $f_{\mathrm{Decay}}(E_i, r(i,t)) < \beta_j$, then the node j is activated with probability $P_R(j) = 2^{\omega_R(1-\beta_R(j)/e_{\mathrm{source}}(t))}$; $\omega_R > 0$ is the probability decay coefficient. Using these parameters, the specific simulation steps of SD-RSNM are described in Appendix A.

To visualize the basic principle of the risk ripple-spreading process, we give a simple example, as shown in Figure 1, where node 0 denotes the contagion source and nodes 1–3 denote normal network nodes, i.e., financial institutions. The energy of a ripple decays as it spreads; i.e., the strength of energy is reflected as the thickness of the ripple.

At $t = 1$, the contagion source, i.e., node 0, first triggers an initial ripple with energy E_0 and spreads out, but it has not yet reached any node.

At $t = 2$, the initial ripple triggered by node 0 reaches node 3. Since $f_{\mathrm{Decay}}(E_0, d_{03}) \geq \beta_3$, node 3 is activated and a directed link from node 0 to node 3 is established. Then, node 3 generates a response ripple with energy $E_3 = \alpha_3 f_{\mathrm{Decay}}(E_0, d_{03})$ that spreads out again.

At $t = 3$, the initial ripple triggered by node 0 reaches node 1. Since $f_{\mathrm{Decay}}(E_0, d_{01}) \geq \beta_1$, node 1 is activated and generates the corresponding response ripple.

At $t = 4$, risk ripples triggered by contagion source disappear; i.e., the energy value decays to 0, while risk ripples triggered by nodes 1 and 3 continue to spread out.

At $t = 5$, the ripple triggered by node 1 reaches node 2; since $f_{\mathrm{Decay}}(E_1, d_{12}) \geq \beta_2$, node 2 is activated by node 1 and generates the corresponding response ripple.

At $t = 6$, the ripple triggered by node 2 reaches node 1, since $f_{\mathrm{Decay}}(E_2, d_{21}) < \beta_1$, node 1 is not activated; the ripple triggered by node 1 reaches node 0, since $f_{\mathrm{Decay}}(E_1, d_{10}) \geq \beta_0$, node 0 is activated by node 1 and generates the corresponding response ripple. At the same time, the ripple triggered by node 1 reaches node 3, although $f_{\mathrm{Decay}}(E_2, d_{21}) < \beta_1$, a dotted link is created from node 1 to 3, which is determined by chance. Then, node 3 generates a response ripple with energy $E_3 = \alpha_3 f_{\mathrm{Decay}}(E_1, d_{13})$.

Thus, a directed financial network consisting of four nodes and five edges is formed.

2.2. Parameter Specifications. Parameter specifications are at the heart of the ripple-spreading network, and in this paper, we set them in the context of systemic risk regime switching. The smooth-transition vector autoregression (STVAR) model proposed by Weise [48] is capable of examining asymmetric mechanisms in both high- and low-state regimes. The general form of the STVAR model can be expressed as follows:

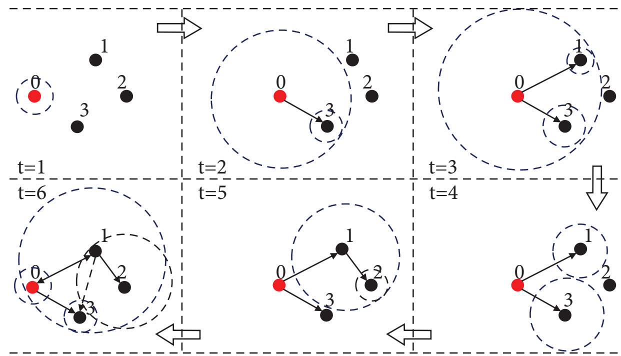

FIGURE 1: A simple example of the semideterministic ripple-spreading network.

$$Y_t = [1 - F(z_{t-1})]\left[\mu_0 + \sum_{k=1}^{p} \Pi_l^k Y_{t-k} + \Gamma X_t\right] + F(z_{t-1})\left[\mu_1 + \sum_{k=1}^{p} \Pi_\mu^k Y_{t-k} + \Xi X_t\right] + \varepsilon_t, \tag{1}$$

$$F(z_t) = \operatorname{diag}\left\{\frac{1}{1 + \exp[-\gamma(z_t - c)]}, \cdots, \frac{1}{1 + \exp[-\gamma(z_t - c)]}\right\}, \quad \gamma > 0, \tag{2}$$

where Y_t is the m-dimensional endogenous variable in the period t, X_t is the q-dimensional exogenous variable in the period t, p is the lag order of the STVAR model, z_t is the state variable, and $F(z_t)$ is the transition function. Given z_t and $F(z_t)$, the sample can be partitioned into two states, a low-state variable regime (l) and a high-state variable regime (h); Π_l^k and Π_μ^k are the k-order lag term coefficient matrices of the endogenous variables in the high- and low-state regimes, respectively. Γ and Ξ are the exogenous variable coefficient matrices; μ_0 and μ_1 are the m-dimensional intercept vectors. $F(z_t)$ is the transition function which takes the form of a logistic function. $F(z_t)$ portrays the probability of a sample being partitioned into different state regimes; diag denotes the diagonal matrix; γ determines the degree of smoothing of the regime transition, the larger the value of γ, the faster the rate of regime transition; c is the threshold parameter for regime partitioning.

Furthermore, (1) can be equated to the following form:

$$Y_t = B_1' W_t + F(z_{t-1}) B_2' W_t + \varepsilon_t, \tag{3}$$

where $B_1 = (\mu_0, \Pi_l^1, \cdots, \Pi_l^p, \Gamma)$, $B_2 = (\mu_1, \Pi_\mu^1, \cdots, \Pi_\mu^p, \Xi)$, $W_t = (1, Y_{t-1}, \cdots, Y_{t-p}, X_t)$, and $\varepsilon_t \sim N(0, \Omega)$.

Following Caggiano et al. [49], the model can be simplified as follows:

$$Y_t = [1 - F(z_{t-1})]\Pi_l Y_{t-1} + F(z_{t-1})\Pi_\mu Y_{t-1} + \varepsilon_t = \Pi_l^* Y_{t-1} + F(z_{t-1})\Pi_\mu^* Y_{t-1} + \varepsilon_t, \tag{4}$$

$$F(z_t) = \{1 + \exp[-\gamma(z_t - c)]\}^{-1}, \quad \gamma > 0, \tag{5}$$

where $\Pi_\mu^* = \Pi_\mu - \Pi_l$, z_t is the normalized state variable, i.e., $z_t = (z_{t0} - z_{\text{mean}})/z_{\text{std}}$, z_{t0} is the original observation, z_{mean} is the mean, and z_{std} is the standard deviation. It should be noted that, in this paper, we use systemic risk measured by CoVaR [50] as the state variable and the risk indicator, i.e., historical volatility [26] of each financial institution as endogenous variables in the model.

On the basis of the coefficient estimation and regime partitioning of the STVAR model, following Diebold et al. [25], we can obtain the variance contribution under high and low systemic risk regimes, i.e., how much of the future uncertainty of variable j is due to shocks in variable i:

$$d_{\text{ij}} = \frac{\sigma_{\text{ii}}^{-1} \sum_{h=0}^{H-1} \left(e_i' A_h \Sigma e_j\right)^2}{\sum_{h=0}^{H-1} \left(e_i' A_h \Sigma A_h' e_i\right)^2}, \tag{6}$$

where d_{ij} denotes the proportion of changes in i caused by the shocks of the endogenous variable j and describes the risk spillover intensity from j to i, N is the number of endogenous variables, H is the forecast period, σ_{ii}^{-1} is the standard deviation of the error term for the i th equation, Σ is the covariance matrix for the error vector ε_t, A_h is the H-step moving average coefficient matrix, and e_i is the selection vector, with one being the i th element and zeros otherwise. Since the shocks between variables are not orthogonal, the entries of each row in the variance decomposition matrix do not add up to 1. Hence, we normalize it according to the row summation approach and obtain

$$\widetilde{d}_{\text{ij}} = \left(\frac{d_{\text{ij}}^H}{\sum_{j=1}^{N} d_{\text{ij}}^H}\right) \times 100. \tag{7}$$

Furthermore, we can set the network parameters based on the results of the regime transformation.

Connection threshold β_i: We assume that the more external shocks an institution is exposed to, the more vulnerable it is to financial contagion. It is similar to $\widetilde{d}_{\mathrm{ij}}$ in the connectedness method proposed by Diebold et al. [25]. Thus, based on (7), the connection threshold for institution i under high and low systemic risk regimes, i.e., $\beta_i(h)$ and $\beta_i(l)$, can be expressed as follows:

$$\beta_i(h) = \frac{1}{\sum_{j=1}^{N}\widetilde{d}_{\mathrm{ij}}(h)}, \quad i \neq j; \beta_i(l) = \frac{1}{\sum_{j=1}^{N}\widetilde{d}_{ij}(l)}, \quad i \neq j. \tag{8}$$

Amplifying factor α_i: We use the market capitalization of each financial institution to specify α_i under high and low systemic risk regimes. For example, the average market capitalization of ICBC under a high-risk regime is 17.014 × 100 billion yuan, so we set $\alpha_{\mathrm{ICBC}}(h) = 17.014$; the average market capitalization of ICBC under a low-risk regime is 16.276 × 100 billion yuan, so we set $\alpha_{\mathrm{ICBC}}(l) = 16.276$.

Spreading speed s_i: Following Xu et al. [43], we use the average turnover rate to specify s_i under different systemic risk regimes. For example, the average turnover rate of ICBC under a high systemic risk regime is 0.081, so we set $s_{ICBC}(h) = 0.081$; the average turnover rate of ICBC under a low systemic risk regime is 0.066, so we set $s_{\mathrm{ICBC}}(l) = 0.066$.

Market distance d_{ij}: d_{ij} is determined by the inverse of the volatility correlation coefficient between institutions i and j; i.e., the higher the correlation between two financial institutions, the shorter their distance and the easier it is for risk ripples to reach. Thus, the market distance between institutions i and j under the high- and low-risk regimes, i.e., $d_{ij}(h)$ and $d_{ij}(l)$, can be expressed as

$$d_{ij}(h) = \frac{1}{\left|\mathrm{cor}_{\mathrm{ij}}(h)\right|}, \mathrm{cor}_{\mathrm{ij}}(h) \neq 0; \; d_{\mathrm{ij}}(h) = \frac{1}{\left|\mathrm{cor}_{\mathrm{ij}}(l)\right|}, \mathrm{cor}_{\mathrm{ij}}(l) \neq 0, \tag{9}$$

where $\mathrm{cor}_{\mathrm{ij}}$ is the correlation coefficient calculated based on history volatility data between institutions i and j. In addition, if $\mathrm{cor}_{\mathrm{ij}} = 0$, then $d_{\mathrm{ij}} = +\infty$.

2.3. Heterogeneous Network. Given a lager enough E_0, the ripple-spreading process will eventually form a stable fully connected network with nodes N and edges $N(N-1)$, which is not conducive to analyzing the systemic importance of financial institutions. Following Xu et al. [43], we use the variance of node degrees to identify the heterogeneous network of the ripple-spreading process under different systemic risk regimes. For every time instant t, let $A^t = (a_{ij}^t), i, j = 1, 2, \cdots, N$ be the adjacency matrix of the instantaneous network in the ripple-spreading process.

The variance of node degrees at t can be expressed as follows:

$$s_t^2 = \frac{\sum_{i=1}^{N}\left(D_i^t - \overline{D}_t\right)^2}{N}, \tag{10}$$

where D_i^t denotes the node degree of the node i, i.e., $D_i^t = \sum_{i=1}^{N} a_{\mathrm{ij}}^t + \sum_{i=1}^{N} a_{\mathrm{ji}}^t$, and $\overline{D}_t$ denotes the average of node degrees, i.e., $\overline{D}_t = (\sum_{i=1}^{N} D_i^t)/N$; when s_t^2 takes the maximum value, the network is of best heterogeneity and appropriate for analyzing systemically important financial institutions (SIFIs).

3. Data

Limited to data availability, we select 55 financial institutions listed before 2011 as the main research object, specifically including 11 real estate companies, 16 banks, 14 securities, 4 insurance, and 10 diversified financial institutions, as shown in Table 1. In terms of sample selection, we include some real estate companies (collectively, financial institutions) in our research sample due to their financial-like attributes. The research sample covers the periods from January 4, 2011, to February 10, 2023. The daily historical volatility [26] of each institution can be expressed as

$$V_{i,t} = 0.511\left(H_{i,t} - L_{i,t}\right)^2 - 0.019\left[\left(C_{i,t} - O_{i,t}\right)\left(H_{i,t} + L_{i,t} - 2O_{i,t}\right) - 2\left(H_{i,t} - O_{i,t}\right)\left(L_{i,t} - O_{i,t}\right)\right] - 0.383\left(C_{i,t} - O_{i,t}\right)^2, \tag{11}$$

where $H_{i,t}, L_{i,t}, O_{i,t}$, and $C_{i,t}$ are the logs of daily high, low, opening, and closing prices, respectively, and the data are obtained from the Wind database.

In the STVAR model with the systemic risk index [50] as the state variable, the results of the grid point search show that the smoothing coefficient γ of the transition function is estimated to be 10 and the parameter c takes the value 1.126. Figure 2(a) shows the results of the transition function. It can be found that the transition function shows a smooth and asymptotic trend, suggesting a nonlinear relationship of asymptotic evolution of risk contagion as the state of systemic risk changes. Furthermore, the distribution of the high and low states of systemic risk over the sample period can be obtained, as shown in Figure 2(b). The shaded areas in Figure 2(b) mark the high systemic risk regime. It can be found that the high systemic risk regime covers the period of

Table 1: *Name and abbreviation of China's financial institutions.

No.	Institution name	Abbr.
1	China Vanke Co., Ltd.	RE01
2	Poly Developments and Holdings Group Co., Ltd.	RE02
3	Shenzhen Overseas Chinese Town Co., Ltd.	RE03
4	China Fortune Land Development Co., Ltd.	RE04
5	Gemdale Corporation	RE05
6	Shanghai Lujiazui Finance & Trade Zone Development Co., Ltd.	RE06
7	Xinhu Zhongbao Co., Ltd.	RE07
8	Oceanwide Holdings Co., Ltd.	RE08
9	Risesun Real Estate Development Co., Ltd.	RE09
10	Youngor Fashion Co., Ltd.	RE10
11	Jinke Property Group Co., Ltd.	RE11
12	Industrial and Commercial Bank of China	ICBC
13	Agricultural Bank of China	ABC
14	Bank of China	BOC
15	China Construction Bank	CCB
16	Bank of Communications	BCM
17	China Merchants Bank	CMB
18	Shanghai Pudong Development Bank	SPD
19	China CITIC Bank	BCC
20	Ping An Bank	PAB
21	Huaxia Bank	HXB
22	China Minsheng Bank	MSB
23	China Everbright Bank	CEB
24	China's Industrial Bank	IBC
25	Bank of Beijing	BOB
26	Bank of Nanjing	BNJ
27	Bank of Ningbo	BNB
28	China Merchants Securities	CMS
29	Changjiang Securities	CJS
30	CITIC Securities	CITIC
31	Everbright Securities	EBS
32	GF Securities	GFS
33	Guoyuan Securities	GYS
34	Sinolink Securities	SLS
35	Southwest Securities	SWS
36	Haitong Securities	HTS
37	Huatai Securities	HZS
38	Northeast Securities	NES
39	Pacific Securities	PS
40	Sealand Securities	SS
41	Industrial Securities	IS
42	China Life Insurance	CLIC
43	China Pacific Insurance	CPIC
44	China Ping An Insurance	PAIC
45	Tianmao Insurance Company	TMIC
46	Xinli Finance	XLF
47	Anxin Trust and Investment	AXT
48	Bohai Leasing	BHL
49	Luxin Venture Capital	LXC
50	Minmetals Capital Company	MCC
51	Minsheng Holdings	MSH
52	Aijian Group	AJG
53	Shaanxi International Trust	SIT
54	Sunny Loan Top	SLT
55	CNPC Capital Company Limited	CNP

**Note*. No. 1–11 represent the real estate companies; no. 12–27 represent banks; no. 28–41 represent securities; no. 42–45 represent insurance; no. 46–55 represent the diversified financial institutions.

"the market liquidity crisis caused by the money shortage in China's banking sector in 2013," "the stock market crash in China in 2015-2016," and the outbreak of the public health event, i.e., "COVID-19" in early 2020. In particular, the aggregation characteristics of systemic risk are the most obvious during the period of "the stock market crash in China in 2015-2016." Since the end of 2014, China's stock market has seen explosive growth and high market sentiment, with investors leveraging into the market through brokerage financing and over-the-counter matching, resulting in an over-leveraged stock market and a serious market valuation bubble. However, by the second half of 2015, the market trend took a sharp turn for the worse, and the departure of leveraged funds accelerated the decline of the stock market, which eventually led to the outbreak of stock disasters and the high fluctuation of systemic risk. Compared with the actual situation, the model constructed in this paper can well identify the evolution of China's systemic risk in various periods, indicating that the logistic smooth-switching model adopted in this paper can effectively identify various types of crisis events, and the estimation results of the model are reasonable and reliable. Finally, it can be estimated that, in the sample range from 2011 to 2023, China's financial system has about 20% of the time in a state of high systemic risk.

On the basis of the above systemic risk regime identification, we give the behavioral parameters of the ripple-spreading network under high and low systemic risk regimes, respectively, as shown in Tables 2 and 3. The market distance, i.e., $d_{\mathrm{ij}}(h)$, $d_{\mathrm{ij}}(l)$, is measured by the inverse of the correlation coefficient of historical volatility between financial institutions. In addition, in China's financial system, the real estate sector occupies an important position, so we set a real estate company as the contagion source to explore the risk ripple-spreading processes. To ensure sufficient network links, the energy of initial ripple of contagion source is set as $e_{\mathrm{source}}(h) = e_{\mathrm{source}}(l) = E_0 = 200\pi$.

4. Results and Discussion

4.1. Ripple-Spreading Process under High Systemic Risk Regimes. Given the model-related parameters mentioned above, we perform the risk ripple-spreading simulation processes under high systemic risk regimes according to the algorithm in Appendix A.

Figure 3 shows the dynamic ripple-spreading processes for 55 financial institutions, by giving some heat maps at $t = 20, 24, 28, 32, 36, 40, 44, 48, 52, 56, 60$, and 64. The rows of the heat maps represent the ripple-spreading effect from a given financial institution to other financial institutions. For example, the first row of Figure 3(a) represents the ripple-spreading effect from the real estate company, i.e., RE01, to other institutions. In addition, in order to better distinguish the ripple-spreading effects within and across sectors, we use dotted lines to partition the heat map by sectors, i.e., the real estate, banking, securities, insurance, and diversified financial sectors. The five diagonal areas of each subfigure in Figure 3 indicate the risk contagion within sectors, and nondiagonal areas indicate the risk cross-contagion between sectors. For example, the top-left corner of Figure 3(a) represents the risk contagion within the real estate sector; the bottom-left corner of Figure 3(a) represents risk cross-contagion from the diversified financial sector to the real estate sector.

From these heat maps, it can be found that the number of contagion links increases gradually over time. By observing the instantaneous state of the ripple-spreading network, we can identify which financial institutions are affected first and which are affected later. On the whole, the contagion triggered by the real estate company, i.e., RE01, first spreads to the real estate and banking sectors and then to the insurance and securities sectors and thus triggers the widespread contagion within the financial system. Specifically, Figures 3(a) and 3(b) show that the financial contagion originating from the source node, i.e., RE01, first reaches the real estate sector (RE02) and the banking sector (ABC, BOC, CCB, BCM, etc.) and then spreads to the insurance sector (CPIC, CLIC, etc.) and the securities sector (GYS). By $t = 24$, as shown in Figure 3(b), all banks are directly affected by the risk ripple of the contagion source. These findings suggest that real estate companies have a significant impact on the financial system, especially on the banking sector. Real estate companies are linked with banks through massive amounts of debt, so when real estate risks occur, the banking sector is affected more deeply and broadly. As risk ripples continue to spread, the cross-contagion occurs among institutions beyond the source node, and the network density increases gradually, as shown in Figures 3(c)–3(l). By $t = 28$, as shown in Figure 3(c), the risk ripple from CCB reaches most banks such as ICBC, ABC, BOC, and BCM. Then, the risk ripple from CCB reaches the securities sector (CMS, CJS, CITIC, etc.) and the insurance sector (CLIC, CPIC, and PAIC), as shown in Figure 3(d). Meanwhile, the risk ripples from securities institutions (CITIC and GYS) begin to spread to the financial system. It is worth noting that, by $t = 32$, all diversified financial institutions are not yet affected by risk ripples and do not send any links to the system, suggesting that diversified financial institutions are more distant from other financial institutions.

From $t = 44$ to $t = 64$, as shown in Figures 3(g)–3(l), we can find that the cross-contagion between financial institutions gradually permeates the entire financial system and the securities sector sends the most risk ripples to the system network. In addition, there are as many as 1,735 links at $t = 52$, which is significantly higher than that at $t = 40$, i.e., 603, indicating that risk ripples among financial institutions spread very fast. After the contagion channels are fully established in the early stage, the rapid risk contagion begins in the later stage. Therefore, it is wise for regulators to take timely measures to block the paths of risk contagion before the contagion channels are fully established.

4.2. Ripple-Spreading Process under Low Systemic Risk Regimes. Given the model-related parameters mentioned above, we perform the risk ripple-spreading simulation

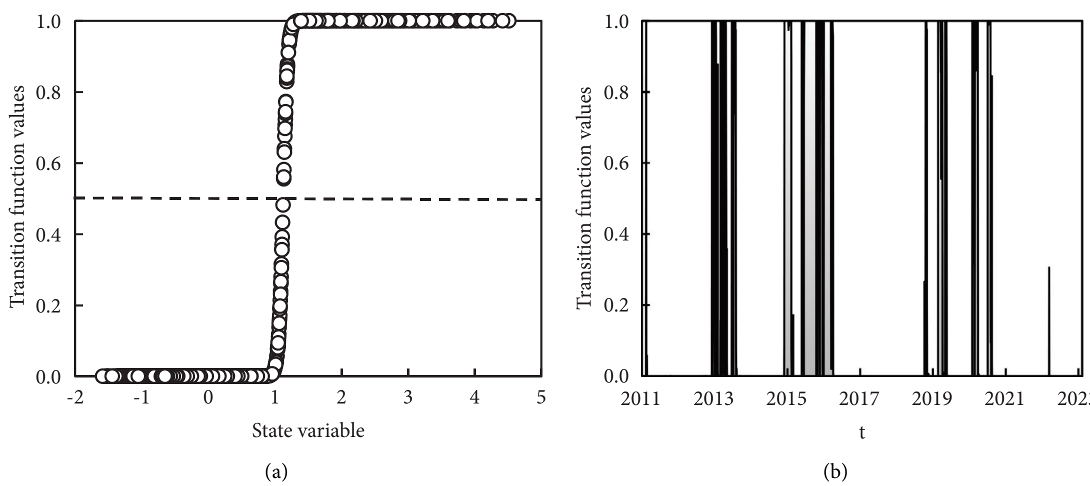

Figure 2: Transition function and state regime transitions. (a) Scatterplot distribution between state variable and the transition function; (b) distribution of sample values of the transition function.

Table 2: Parameters of the ripple-spreading network: high systemic risk regime.

	RE01	RE02	RE03	RE04	RE05	RE06	RE07	RE08	RE09	RE10	RE11
α_i	2.546	1.288	0.589	0.772	0.550	0.611	0.367	0.432	0.362	0.336	0.270
β_i	1.233	1.066	1.067	1.085	1.071	1.076	1.097	1.074	1.079	1.070	1.093
s_i	0.966	0.995	1.196	0.583	0.758	0.451	0.958	0.352	0.935	1.012	1.529
	ICBC	ABC	BOC	CCB	BCM	CMB	SPD	BCC	PAB	HXB	MSB
α_i	17.014	11.060	10.210	12.657	4.026	5.947	3.343	2.721	1.988	1.145	2.936
β_i	1.057	1.066	1.057	1.057	1.061	1.066	1.070	1.054	1.050	1.063	1.073
s_i	0.081	0.106	0.143	1.263	0.415	0.354	0.395	0.209	0.651	0.526	0.487
	CEB	IBC	BOB	BNJ	BNB	CMS	CJS	CITIC	EBS	GFS	GYS
α_i	1.893	3.304	1.252	0.623	0.852	1.093	0.488	2.290	0.655	1.159	0.368
β_i	1.069	1.063	1.071	1.059	1.068	1.050	1.055	1.052	1.057	1.046	1.052
s_i	0.414	0.632	0.559	1.003	0.848	0.733	1.416	1.957	1.294	1.043	1.848
	SLS	SWS	HTS	HZS	NES	PS	SS	IS	CLIC	CPIC	PAIC
α_i	0.377	0.393	1.553	1.376	0.261	0.293	0.281	0.508	6.929	2.602	9.373
β_i	1.062	1.055	1.053	1.049	1.060	1.065	1.053	1.058	1.076	1.064	1.065
s_i	2.103	1.427	1.336	1.296	2.506	3.344	2.597	1.634	0.120	0.444	0.870
	TMIC	XLF	AXT	BHL	LXC	MCC	MSH	AJG	SIT	SLT	CNP
α_i	0.276	0.053	0.299	0.324	0.168	0.169	0.044	0.173	0.174	0.041	0.447
β_i	1.112	1.222	1.104	1.061	1.104	1.096	1.371	1.403	1.082	1.109	1.101
s_i	1.602	1.732	1.868	0.860	2.404	3.004	2.676	1.724	2.133	3.873	1.436

Note. The data in Table 2 are compiled by the authors based on Chapter 2.2.

processes under low systemic risk regimes according to the algorithm in Appendix A.

For a better comparative analysis with the ripple-spreading network under high systemic risk regimes, Figure 4 similarly shows heat maps of the ripple-spreading process under the low systemic risk regime at $t = 20$, 24, 28, 32, 36, 40, 44, 48, 52, 56, 60, and 64. From these heat maps, we find that the contagion triggered by the contagion source, i.e., RE01, first spreads to the real estate sector and then to the banking, securities, and insurance sectors and thus triggers the cross-contagion beyond the source node. Specifically, Figures 4(a)–4(c) show that the financial contagion originating from the source node, i.e., RE01, first reaches the real estate sector (RE02, RE03, RE05, etc.) and then spreads to the banking sector (ICBC, ABC, CCB, etc.), the securities sector (CJS, CITIC, GFS, etc.), and the insurance sector (CPIC, PAIC). By $t = 28$, as shown in Figure 4(c), most banks are directly affected by the source node, which is similar to the ripple-spreading network under high systemic risk regimes; i.e., the real estate sector has the most significant impact on the banking sector. Moreover, by $t = 28$, the number of links in the system network is 32, which is smaller than the links under the high systemic risk regime, suggesting that financial institutions are relatively more distant from each other under low systemic risk regimes. As the risk ripple-spreading process goes on, we find that the cross-contagion occurs beyond the source node, as shown in Figures 4(d)–4(f). By $t = 32$, the cross-contagion occurs

Table 3: Parameters of the ripple-spreading network: low systemic risk regime.

	RE01	RE02	RE03	RE04	RE05	RE06	RE07	RE08	RE09	RE10	RE11
α_i	2.045	1.302	0.531	0.453	0.453	0.396	0.293	0.252	0.277	0.273	0.237
β_i	1.137	1.119	1.156	1.317	1.141	1.330	1.259	1.191	1.211	1.126	1.347
s_i	0.889	0.925	1.148	1.334	0.998	0.371	0.604	0.441	1.126	0.597	1.620
	ICBC	ABC	BOC	CCB	BCM	CMB	SPD	BCC	PAB	HXB	MSB
α_i	16.276	10.272	9.095	12.717	3.520	6.591	2.542	2.260	2.026	0.907	2.258
β_i	1.102	1.088	1.100	1.103	1.081	1.073	1.072	1.110	1.099	1.075	1.079
s_i	0.066	0.148	0.085	0.930	0.316	0.369	0.487	0.135	0.832	0.483	0.466
	CEB	IBC	BOB	BNJ	BNB	CMS	CJS	CITIC	EBS	GFS	GYS
α_i	1.620	3.040	0.996	0.613	1.086	1.025	0.360	2.222	0.555	1.040	0.303
β_i	1.074	1.081	1.088	1.100	1.105	1.072	1.080	1.068	1.101	1.086	1.108
s_i	0.396	0.637	0.434	0.769	0.693	0.602	1.053	1.277	1.089	0.996	1.218
	SLS	SWS	HTS	HZS	NES	PS	SS	IS	CLIC	CPIC	PAIC
α_i	0.306	0.288	1.228	1.053	0.194	0.205	0.228	0.434	6.527	2.367	8.106
β_i	1.131	1.149	1.076	1.072	1.078	1.106	1.114	1.084	1.111	1.100	1.089
s_i	1.876	0.738	1.001	1.061	1.398	2.135	3.518	1.469	0.103	0.473	0.801
	TMIC	XLF	AXT	BHL	LXC	MCC	MSH	AJG	SIT	SLT	CNP
α_i	0.180	0.042	0.215	0.196	0.119	0.211	0.033	0.130	0.122	0.034	0.595
β_i	1.477	2.449	1.217	1.300	1.319	1.340	2.179	1.175	1.113	1.292	1.706
s_i	1.146	3.146	1.362	1.175	1.144	2.138	2.019	1.604	1.754	2.699	0.839

Note. The data in Table 3 are compiled by the authors based on Chapter 2.2.

within the securities sector, and some securities institutions such as CITIC begin to send risk ripples or links to the banking sector. By $t = 36$, the risk cross-contagion occurs within the banking sector. In addition, by $t = 40$, we can find that most of the links constructed by the diversified financial institutions are mostly from securities institutions, while the diversified financial institutions do not issue any links to the system network. This implies that the diversified financial institutions are the main receiver of risk ripples in the Chinese financial system. From $t = 44$ to $t = 64$, as shown in Figures 4(g)–4(l), we find that the risk cross-contagion relationships become more complex and the network density increases gradually. Taken together, although risk ripples spread slower in low than in high systemic risk regimes, systemic shocks can also trigger large-scale risk contagion within the financial system even in low systemic risk regime as risk ripples spread.

4.3. Network Centrality Analysis of Heterogeneous Networks. In the above analysis, we have studied the dynamic ripple-spreading processes in China's financial system under high and low systemic risk regimes. Furthermore, we discuss the network centrality of heterogeneous ripple-spreading networks and identify the systemic importance of financial institutions (SIFIs). According to (10), each process can generate a stable heterogeneous network. We set the upper time limit to $t = 500$. Figure 5 shows the dynamic change trend of network heterogeneity. It can be seen that network heterogeneity increases sharply from 0 to a maximum value and then decreases gradually as risk ripples spread. The network heterogeneity in high and low systemic risk regimes reaches its maximum value at $t = 49$ and $t = 60$, respectively.

In this subsection, we consider four network centrality indicators, i.e., degree centrality (DC), closeness centrality (CC), eigenvector centrality (EC), and betweenness centrality (BC), based on heterogeneous networks selected above under different risk regimes, to identify and analyze SIFIs. These four network centrality indicators measure the systemic importance of financial institutions from different perspectives. In general, the higher the network centrality of a node, the higher its systemic importance in the system network. The implications of these four centralities are presented in Appendix A. Figures 6–9 show the measurement results of four network centrality indicators for each financial institution under high and low systemic risk regimes. The results are given in the form of heat maps, where darker colors indicate higher centrality values and higher systemic importance of financial institutions. Due to space constraints, only some of the English abbreviations of financial institutions are shown in heat maps, and their order from left to right is consistent with Table 1. As can be seen, whether the financial system is in a high- or low-risk regime, nodes with higher network centrality are mostly distributed in the securities, banking, and real estate sectors, and nodes with lower network centrality are mostly distributed in the diversified financial sector.

Specifically, Table 4 shows the top 15 SIFIs ranked based on four network centralities under high and low systemic risk regimes. Overall, the top 15 SIFIs are concentrated in the banking and securities sectors. However, there are some differences in the ranking of financial institutions under high and low risk regimes. In particular, the systemic importance characteristics of some securities institutions in the high systemic risk regime are particularly significant. For example, securities institutions such as GYS, HZS, IS, and GFS all appear in the top 15 lists for four centralities under high systemic risk regimes and only appear in the top 15 lists for one or two centralities under low systemic risk regimes. In addition, some real estate companies, such as RE02, RE09, and RE10, appear in the top 15 lists, while diversified

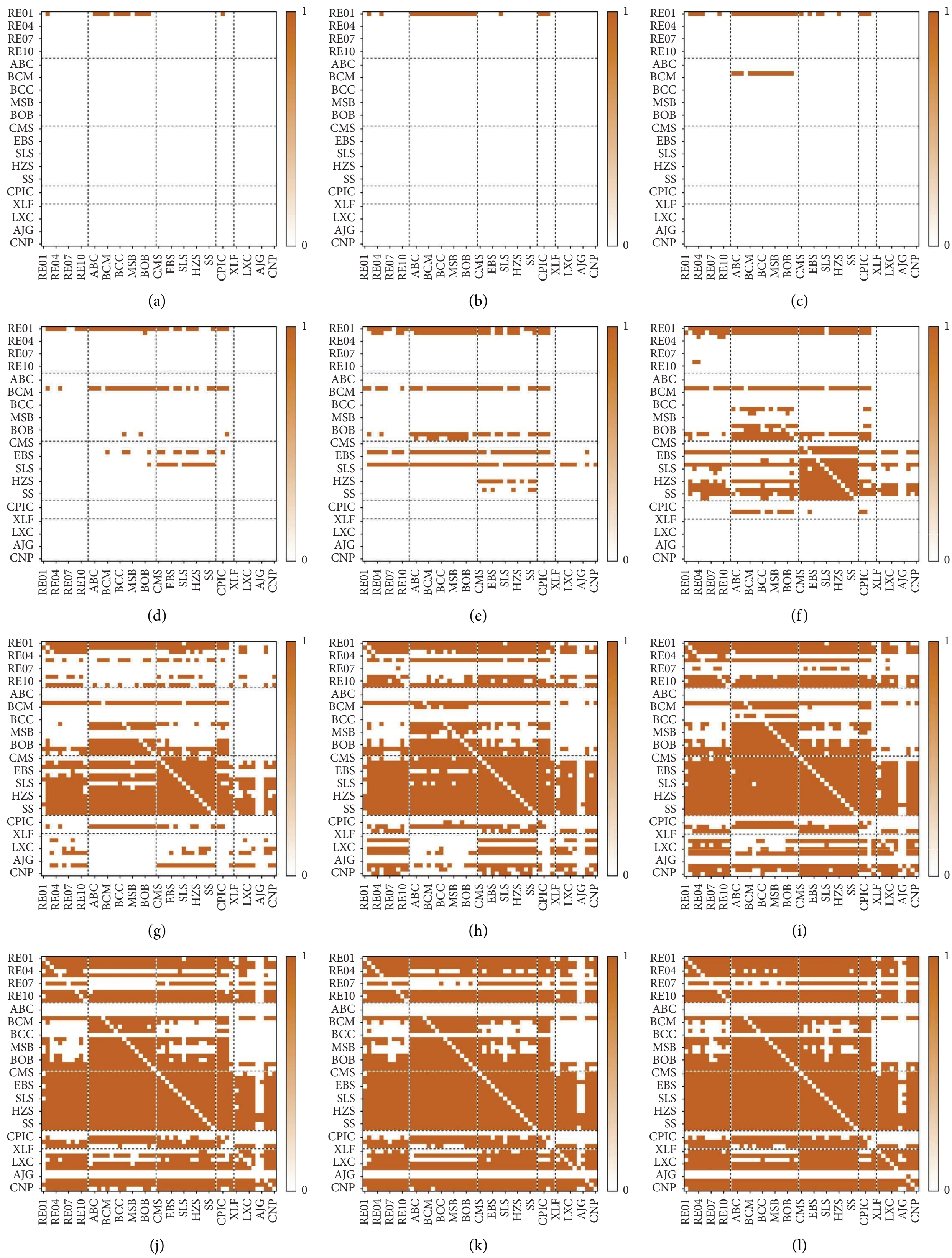

Figure 3: Heat maps for dynamic ripple-spreading process under high systemic risk regimes. Due to space constraints, only some of the English abbreviations of financial institutions are shown, and their order from top to bottom and from left to right is consistent with Table 1. (a) Current time: $t = 20$, links: 14; (b) current time: $t = 24$, links: 22; (c) current time: $t = 28$, links: 43; (d) current time: $t = 32$, links: 97; (e) current time: $t = 36$, links: 251; (f) current time: $t = 40$, links: 603; (g) current time: $t = 44$, links: 1040; (h) current time: $t = 48$, links: 1477; (i) current time: $t = 52$, links: 1735; (j) current time: $t = 56$, links: 1911; (k) current time: $t = 60$, links: 2041; (l) current time: $t = 64$, links: 2134.

Figure 4: Heat maps for the dynamic ripple-spreading process under low systemic risk regimes. Due to space constraints, only some of the English abbreviations of financial institutions are shown, and their order from top to bottom and from left to right is consistent with Table 1. (a) Current time: $t = 20$, links: 3; (b) current time: $t = 24$, links: 17; (c) current time: $t = 28$, links: 32; (d) current time: $t = 32$, links: 74; (e) current time: $t = 36$, links: 227; (f) current time: $t = 40$, links: 487; (g) current time: $t = 44$, links: 752; (h) current time: $t = 48$, links: 953; (i) current time: $t = 52$, links: 1144; (j) current time: $t = 56$, links: 1342; (k) current time: $t = 60$, links: 1532; (l) current time: $t = 64$, links: 1733.

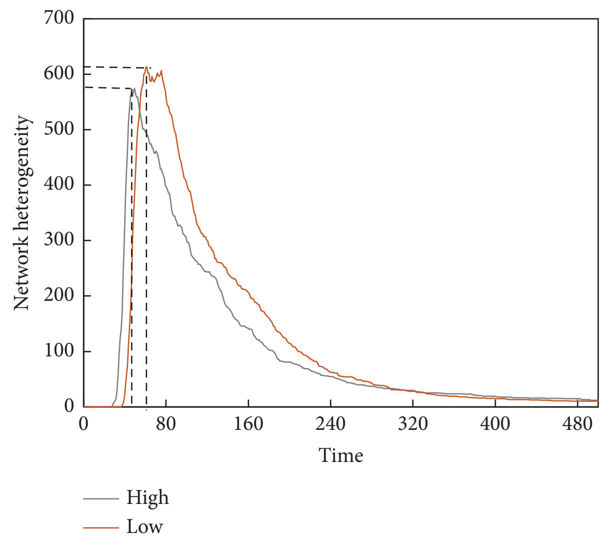

FIGURE 5: Changes in network heterogeneity with the spread of risk ripples. “High” denotes the high systemic risk regime. “Low” denotes the low systemic risk regime.

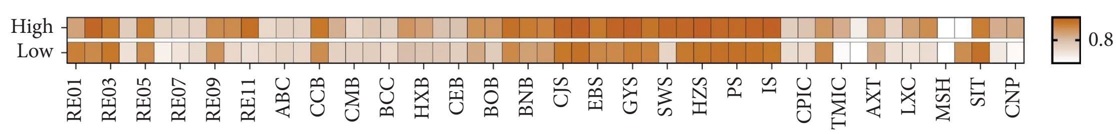

FIGURE 6: Heat map of degree centrality for each financial institution.

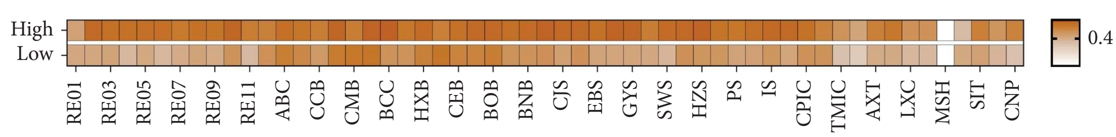

FIGURE 7: Heat map of closeness centrality for each financial institution.

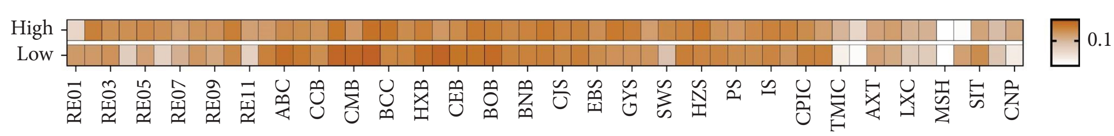

FIGURE 8: Heat map of eigenvector centrality for each financial institution.

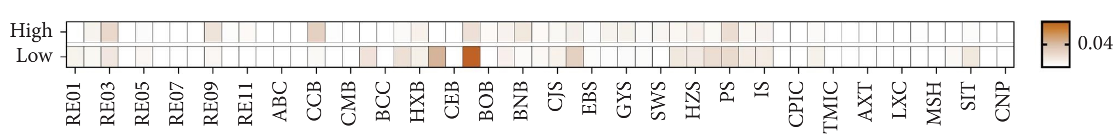

FIGURE 9: Heat map of betweenness centrality for each financial institution.

financial institutions do not appear in the top 15 lists. Therefore, we conclude that most securities and banks and some real estate companies have the highest systemic importance, and the diversified financial institutions have the lowest importance. Furthermore, we average the network centrality indicators for each financial institution by sector to obtain a systemic importance ranking for each sector, and the results are shown in Table 5. It can be found that the systemic importance of the real estate sector is higher in high than in low systemic risk regimes, and supervisors should pay particular attention to the risk contagion capacity of the real estate sector when the financial system is under pressure. In addition, whether the financial system is in a high or low systemic risk regime, the securities sector has the highest “degree centrality” and “betweenness centrality,” which indicates that the securities sector not only has significant risk ripple linkage capacity but also has significant risk ripple intermediation effects. The spreading of risk ripples relies

Table 4: The top 15 SIFIs under high and low systemic risk regimes.

Rank	High systemic risk regime				Low systemic risk regime			
	DC	CC	EC	BC	DC	CC	EC	BC
1	GYS	BCC	SPD	CCB	CITIC	MSB	SPD	IBC
2	HZS	HZS	BCC	RE03	NES	SPD	MSB	MSB
3	CITIC	GFS	BCM	PS	PS	CMB	BCM	CITIC
4	IS	CMS	HZS	IBC	SIT	BCM	CMB	PS
5	GFS	SPD	GFS	RE09	SS	BOB	BOB	NES
6	SS	GYS	CMS	BNB	HZS	ABC	HXB	PAB
7	RE02	RE10	IBC	CITIC	RE03	HXB	ABC	SPD
8	CJS	BCM	BOB	HZS	CJS	IBC	IBC	SIT
9	SWS	CITIC	GYS	HXB	IS	CEB	CEB	RE03
10	HTS	IS	RE10	GYS	HTS	BOC	BOC	HTS
11	NES	RE02	HXB	BNJ	GYS	CITIC	HTS	HZS
12	PS	CJS	CITIC	IS	RE01	HTS	CITIC	IS
13	RE11	HTS	RE02	GFS	SLS	CMS	CMS	SS
14	BNJ	IBC	IS	RE02	EBS	ICBC	CPIC	HXB
15	SLS	BOB	HTS	SWS	RE02	CPIC	ICBC	BNJ

Table 5: Systemic importance ranking of financial sectors under high and low systemic risk regimes.

Rank	High systemic risk regime				Low systemic risk regime			
	DC	CC	EC	BC	DC	CC	EC	BC
1	G3	G3	G3	G3	G3	G2	G2	G3
2	G1	G2	G2	G2	G1	G3	G3	G2
3	G2	G1	G1	G1	G2	G4	G4	G1
4	G4	G4	G4	G4	G4	G1	G1	G4
5	G5	G5	G5	G5	G5	G5	G5	G5

Note. G1, G2, G3, G4, and G5 represent the real estate, banking, securities, insurance, and diversified financial sectors, respectively.

heavily on information transmission from the securities sector, thus providing a new entry point for blocking risk contagion.

5. Conclusion

In this paper, we propose using the ripple-spreading network model to reveal the spatiotemporal evolutionary characteristics of systemic risk contagion in China's financial system. Compared to existing financial networks such as correlation networks and spillover networks, the ripple-spreading network provides a new tool for modeling the dynamic process of how financial contagion spreading from the contagion source to the whole financial system. On the one hand, the dynamic ripple-spreading process can reveal which nodes are affected first and which are affected later. On the other hand, we can identify SIFIs based on the generated heterogeneous networks.

As for the dynamic ripple-spreading processes, we find that risk ripples spread much faster in high than in low systemic risk regimes. However, systemic shocks can also trigger large-scale risk contagion within the financial system even in low systemic risk regimes as the risk ripples continue. Excessive network connectedness among institutions can amplify financial shocks through contagion effects. Overall, whether the financial system is in a high- or low-risk regime, the risk ripples from the contagion source (i.e., a real estate company) spread first to the real estate sector and the banking sector. On the one hand, institutions belonging to the same sector share similarities in terms of their business scope, business pattern, investment pattern, risk management, and financial regulation, etc., which may make it easier for the cross-contagion to occur within the sector. On the other hand, the real estate companies are linked with banks through massive amounts of debt, so when real estate risks occur, the banking sector is affected more deeply and broadly. In addition, the diversified financial institutions have fewer risk interactions in the early stage, and all the links established by the diversified institutions are mostly from securities, while it issues fewer links to the system network. This implies that the diversified institutions are the main receiver of risk ripples in the Chinese financial system.

As for the identification for SIFIs, we find that most securities and banks and some real estate companies are the most systemically important financial institutions in China's financial system. Although we set the real estate company, i.e., RE01, as the contagion source, securities institutions exhibit the strongest risk ripple-spreading ability as the risk ripples continue, sending the most links to the system network. Especially, the systemic importance characteristics of securities institutions in high systemic risk regimes are particularly significant. To some extent, the results are not consistent with the previous studies, which noted that large financial institutions such as banks and insurances are the most SIFIs [51, 52]. For example, Wang et al. [51] noted that banks and insurance institutions in China contribute more to systemic risk than securities institutions. Chen et al. [52] pointed out that SIFIs are concentrated in the banking and insurance sectors. The reason for this is that the methods used in these studies focus mainly on assessing the systemic risk contribution of financial institutions. The higher the systemic risk contribution of a financial institution, the higher the level of systemic importance. However, the measurement of systemic risk contribution usually takes into account the impact of the size of financial institutions, so that large-scale financial institutions such as banks and insurance are identified as SIFI. Our paper mainly focuses on the network correlation of financial contagion, rather than the systemic risk contribution. Financial institutions with the highest network correlation tend to have the highest systemic importance. At the same time, this inconsistency reminds financial regulators and government departments that systemic risk regulation should focus not only on large institutions but also on institutions with strong ripple-spreading effects.

Finally, it is worth noting that the channel mechanism of financial contagion is very complex, this paper only analyzes the dynamic ripple-spreading processes of risk triggered by contagion source under high and low systemic risk regimes and does not involve the exploration of specific contagion channels or mechanisms. In the future, a more comprehensive integration of the factors affecting financial contagion will provide a better understanding of the contagion process of risks.

Appendix

A. Simulation Steps of the Ripple-Spreading Network

Given the ripple-spreading network behavior parameters, the new dynamic ripple-spreading network model can be mathematically described as follows:

Step 1. Initialize the current time instant, i.e., $t = 0$; initialize the current point energy of contagion source as $e_{\text{source}}(t) = E_0$, $(E_0 > 0)$; initialize the current point energy of each network node as $e_{\text{nodes}}(i,t) = E_{\text{nodes}}(i) = 0, i = 1, 2, \cdots, N$. Assume contagion source and each node have a ripple with a current radius of 0, i.e., $r_{\text{source}}(t) = 0$, $r_{\text{nodes}}(i,t) = 0$.

Step 2. If the stopping criteria are not satisfied, do the following:

Step 2.1. Let $t = t + 1$,

Step 2.2. Update the current radius and point energy of contagion source as $r_{\text{source}}(t) = r_{\text{source}}(t-1) + s_0$, $e_{\text{source}}(t) = f_{\text{Decay}}(E_0, r_{\text{source}}(t))$, where s_0 is the spreading speed of contagion source, i.e., the change in the radius of a ripple during one time instant, f_{Decay} is a function defining how the point energy decays as the ripple spreads out. A typical decaying function can be defined as follows:

$$f_{\text{Decay}}(E_0, r_{\text{source}}(t)) = \frac{\eta E_0}{2\pi r_{\text{source}}(t)}, \tag{A.1}$$

where η is a decaying coefficient and π is the mathematical constant. Clearly, η has an important influence on the decaying speed of ripples and will therefore affect the final network topology. In this paper, following Xu et al. [43], we set $\eta = 1$.

Step 2.3. Check which new nodes are reached by the ripples of contagion source. Suppose d_{0j} is the distance between the contagion source and node j. If $d_{0j} \le r_{\text{source}}(t)$ and $e_{\text{source}}(t) \ge \beta_j$, then node j is activated by contagion source, and thus, a link from the contagion source to node j is established. Node j generates a responding ripple with initial energy $E_{\text{nodes}}(j) = \alpha_j e_{\text{source}}(t)$ and $e_{\text{nodes}}(j,t) = E_{\text{nodes}}(j)$. In this step, we consider the uncertainty characteristics of financial risk contagion; i.e., if $d_{0j} \le r_{\text{source}}(t)$ and $e_{\text{source}}(t) < \beta_j$, then node j generates responding ripple with the following probability:

$$P_R(j) = 2^{\omega_R\left(1-\beta_R(j)/e_{\text{source}}(t)\right)}, \tag{A.2}$$

where $\omega_R > 0$ is the probability decay coefficient. Obviously, the lower the ripple energy, the lower the probability of generating node behavior.

Step 2.4. If $e_{\text{nodes}}(i, t-1) > 0$, then update the current radius and energy of the ripple starting from node i in a similar way to the ripple from the contagion source, i.e., $r_{\text{nodes}}(i,t) = r_{\text{nodes}}(i,t-1) + s_i$; $e_{\text{nodes}}(i,t) = f_{\text{Decay}}(E_{\text{nodes}}(i), r_{\text{nodes}}(i,t))$

Step 2.5. Check which new nodes are reached by the ripples of nodes. If $d_{\text{ij}} \le r_{\text{nodes}}(i,t)$ and $e_{\text{nodes}}(i,t) \ge \beta_j$, then node j is activated by node i, and thus, a directed link from node i to node j is established. Node j generates a responding ripple with initial energy $E_{\text{nodes}}(j) = \alpha_j e_{\text{nodes}}(i,t)$ and $e_{\text{nodes}}(j,t) = E_{\text{nodes}}(j)$. Likewise, we consider the uncertainty characteristics of financial risk contagion; i.e., if $d_{\text{ij}} \le r_{\text{nodes}}(i,t)$ and $e_{\text{nodes}}(i,t) < \beta_j$, then node j generates responding ripple with the probability shown in equation (A.2).

Finally, we can stop the simulation in Step 2 by setting an upper time limit.

B. Networks Centrality Measures

The degree centrality of node i can be expressed as follows:

$$\text{DC}(i) = \frac{\left(\sum_{j=1}^{N} a_{\text{ij}} + \sum_{j=1}^{N} a_{\text{ji}}\right)}{(N-1)}, \tag{B.1}$$

where N is the number of nodes and $N-1$ is the maximum out- or in-degree. If there is a directed link from node i to j, $a_{\text{ij}} = 1$; otherwise, $a_{\text{ij}} = 0$.

The closeness centrality for node i is calculated as follows:

$$\text{CC}(i) = \frac{(N-1)}{\sum_{j=1, j\ne i}^{N} d_{\text{ij}}}, \tag{B.2}$$

where d_{ij} denotes the length of a shortest directed path from i to j.

Eigenvector centrality is a global measure of network centrality. It assigns a relative score to each node in the network, and in the contribution of a given node's score, connections to nodes with high scores are larger than connections to nodes with low scores. The relative centrality score for node i can be defined as

$$x_i = \frac{\left(\sum_{j=1}^{N} a_{\text{ij}} x_j\right)}{\lambda}, \tag{B.3}$$

where λ is a constant. It can be written as an eigenvector equation: $Ax = \lambda x$. Typically, each eigenvector will correspond to a different eigenvalue λ. Only the solution corresponding to the largest eigenvalue is required by the centrality measure.

The betweenness centrality for node i is calculated as follows:

$$\mathrm{BC}(i) = \frac{\left(\sum_{j,k}\sigma_{\mathrm{jk}}(i)/\sigma_{jk}\right)}{(n-1)(n-2)}, \tag{B.4}$$

where $i \neq j$, $j \neq k$ is the number of shortest directed paths linking j and k and $\sigma_{\mathrm{jk}}(i)$ is the number of shortest directed paths linking j and k that contain node i.

Data Availability

The data used to support the findings of this study are available from the corresponding authors upon request.

Conflicts of Interest

The authors declare that they have no conflicts of interest.

Acknowledgments

This work was supported by the National Statistical Science Research Project (Grant no. 2023LY098).

References

[1] G. J. Wang, H. B. Si, Y. Y. Chen, C. Xie, and J. Chevallier, "Time domain and frequency domain Granger causality networks: application to China's financial institutions," *Finance Research Letters*, vol. 39, 2021.

[2] B. B. Zhang, X. M. Xie, and C. M. Li, "How connected is China's systemic financial risk contagion network?--A dynamic network perspective analysis," *Mathematics*, vol. 11, no. 10, p. 2267, 2023.

[3] V. V. Acharya, L. H. Pedersen, T. Philippon, and M. Richardson, "Measuring systemic risk," *Review of Financial Studies*, vol. 30, no. 1, pp. 2–47, 2017.

[4] T. Adrian and M. K. Brunnermeier, "CoVaR," *The American Economic Review*, vol. 106, no. 7, pp. 1705–1741, 2016.

[5] D. Morelli and D. Vioto, "Assessing the contribution of China's financial sectors to systemic risk," *Journal of Financial Stability*, vol. 50, 2020.

[6] N. Borri and G. D. Giorgio, "Systemic risk and the COVID challenge in the European banking sector," *Journal of Banking & Finance*, vol. 140, 2022.

[7] Z. S. Ouyang, X. T. Yang, and Y. Huang, "Research on systemic risk contagion effect of Chinese financial institutions considering network public opinion index," *Chinese Journal of Management Science*, vol. 30, no. 4, pp. 1–12, 2022.

[8] Y. J. Duan, S. El Ghoul, O. Guedhami, H. Li, and X. Li, "Bank systemic risk around COVID-19: a cross-country analysis," *Journal of Banking & Finance*, vol. 133, 2021.

[9] B. J. Zhang, S. Y. Wang, Y. J. Wei et al., "Measuring the systemic risk contribution of financial institutes in China based on CoES model," *Systems Engineering-Theory & Practice*, vol. 38, no. 3, pp. 565–575, 2018.

[10] S. W. Chen, L. Guo, and W. K. Zhang, "Financial risk measurement and spatial spillover effects based on an imported financial risk network: evidence from countries along the belt and road," *Mathematics*, vol. 11, no. 6, p. 1349, 2023.

[11] C. Brownlees and R. F. Engle, "SRISK: a conditional capital shortfall measure of systemic risk," *Review of Financial Studies*, vol. 30, no. 1, pp. 48–79, 2017.

[12] E. Goldman, "Uncertainty in systemic risks rankings: bayesian and frequentist analysis," *SSRN Electronic Journal*, vol. 56, 2023.

[13] C. Jiang, Q. Sun, T. L. Ye, and Q. Wang, "Identification of systemically important financial institutions in a multiplex financial network: a multi-attribute decision-based approach," *Physica A: Statistical Mechanics and its Applications*, vol. 611, 2023.

[14] S. Martinez-Jaramillo, B. Alexandrova-Kabadjova, B. Bravo-Benitez, and J. P. Solórzano-Margain, "An empirical study of the Mexican banking system's network and its implications for systemic risk," *Journal of Economic Dynamics and Control*, vol. 40, pp. 242–265, 2014.

[15] M. R. Borges, L. Ulica, and M. Gubareva, "Systemic risk in the Angolan interbank payment system-A network approach," *Applied Economics*, vol. 52, no. 45, pp. 4900–4912, 2020.

[16] E. Denbee, C. Julliard, Y. Li, and K. Yuan, "Network risk and key players: a structural analysis of interbank liquidity," *Journal of Financial Economics*, vol. 141, no. 3, pp. 831–859, 2021.

[17] L. X. Sun, "Financial networks and systemic risk in China's banking system," *Finance Research Letters*, vol. 34, 2020.

[18] Q. Shi, X. Q. Sun, and Y. L. Jiang, "Concentrated commonalities and systemic risk in China's banking system: a contagion network approach," *International Review of Financial Analysis*, vol. 83, 2022.

[19] V. Boginski, S. Butenko, and P. M. Pardalos, "Mining market data: a network approach," *Computers & Operations Research*, vol. 33, no. 11, pp. 3171–3184, 2006.

[20] F. Aslam, Y. T. Mohmand, P. Ferreira, B. A. Memon, M. Khan, and M. Khan, "Network analysis of global stock markets at the beginning of the coronavirus disease (Covid-19) outbreak," *Borsa Istanbul Review*, vol. 20, pp. S49–S61, 2020.

[21] G. Nicola, P. Cerchiello, and T. Aste, "Information network modeling for US banking systemic risk," *Entropy*, vol. 22, no. 11, p. 1331, 2020.

[22] M. Billio, M. Getmansky, A. W. Lo, and L. Pelizzon, "Econometric measures of connectedness and systemic risk in the finance and insurance sectors," *Journal of Financial Economics*, vol. 104, no. 3, pp. 535–559, 2012.

[23] X. Cui and L. Yang, "Systemic risk and idiosyncratic networks among global systemically important banks," *International Journal of Finance & Economics*, vol. 29, no. 1, pp. 58–75, 2022.

[24] Y. Q. Dong and Z. J. Dong, "An innovative approach to analyze financial contagion using Causality-based complex network and value at risk," *Electronics*, vol. 12, no. 8, p. 1846, 2023.

[25] F. X. Diebold and K. Yilmaz, "On the network topology of variance decompositions: measuring the connectedness of financial firms," *Journal of Econometrics*, vol. 182, no. 1, pp. 119–134, 2014.

[26] M. Demirer, F. X. Diebold, L. Liu, and K. Yilmaz, "Estimating global bank network connectedness," *Journal of Applied Econometrics*, vol. 33, no. 1, pp. 1–15, 2018.

[27] X. Yang, S. Chen, H. Liu, X. Yang, and C. Huang, "Jump volatility spillover network based measurement of systemic importance of Chinese financial institutions," *International*

Journal of Finance & Economics, vol. 28, no. 2, pp. 1201–1213, 2023.

[28] W. K. Härdle, W. Wang, and L. Yu, "TENET: tail-Event driven NETwork risk," *Journal of Econometrics*, vol. 192, no. 2, pp. 499–513, 2016.

[29] Y. Deng and C. Y. Gao, "Where does the risk lie? Systemic risk and tail risk networks in the Chinese financial market," *Pacific Economic Review*, vol. 28, no. 2, pp. 167–190, 2023.

[30] G. Bonaccolto, M. Caporin, and R. Panzica, "Estimation and model-based combination of causality networks among large US banks and insurance companies," *Journal of Empirical Finance*, vol. 54, no. 5, pp. 1–21, 2019.

[31] Y. W. Xie, F. Jiao, S. A. Li, Q. Liu, and Y. Tse, "Systemic Risk in financial institutions: a multiplex network approach," *Pacific-Basin Finance Journal*, vol. 73, 2022.

[32] A. H. Elsayed, N. Naifar, G. S. Uddin, and G. J. Wang, "Multilayer information spillover networks between oil shocks and banking sectors: evidence from oil-rich countries," *International Review of Financial Analysis*, vol. 87, 2023.

[33] F. Wu, X. Q. Xiao, X. Zhou, D. Zhang, and Q. Ji, "Complex risk contagions among large international energy firms: a multi-layer network analysis," *Energy Economics*, vol. 114, 2022.

[34] Z. F. Dai, R. Tang, and X. H. Zhang, "Multilayer network analysis for measuring the inter-connectedness between the oil market and G20 stock markets," *Energy Economics*, vol. 120, 2023.

[35] X. B. Hu, M. Wang, M. S. Leeson, E. L. Hines, and E. Di Paolo, "Deterministic ripple-spreading model for complex networks," *Physical Review*, vol. 83, no. 4, 2011.

[36] T. Back, U. Hammel, and H. P. Schwefel, "Evolutionary computation: comments on the history and current state," *IEEE Transactions on Evolutionary Computation*, vol. 1, no. 1, pp. 3–17, 1997.

[37] R. Alfattani, M. Yunus, T. Alamro, and I. A. Alnaser, "Multiresponse optimization of linkage parameters of a compliant mechanism using hybrid genetic algorithm-based swarm intelligence," *Computational Intelligence and Neuroscience*, vol. 2021, Article ID 4471995, 17 pages, 2021.

[38] D. W. Cheng, Z. B. Niu, and J. Li, "Regulating systemic crises: stemming the contagion risk in networked-loans through deep graph learning," *IEEE Transactions on Knowledge and Data Engineering*, vol. 35, no. 6, pp. 6278–6289, 2023.

[39] H. Li and N. Y. Shi, "Application of genetic optimization algorithm in financial portfolio problem," *Computational Intelligence and Neuroscience*, vol. 2022, Article ID 5246309, 9 pages, 2022.

[40] X. B. Hu, M. Wang, and M. S. Leeson, "Ripple-spreading network model optimization by genetic algorithm," *Mathematical Problems in Engineering*, vol. 2013, Article ID 176206, 15 pages, 2013.

[41] J. C. Hull, "Risk Management and Financial Institutions," *Wiley Finance Series*, Wiley, NJ, USA, 2015.

[42] Z. Su and F. W. Xu, "Dynamic identification of systemically important financial markets in the spread of contagion: a ripple network based collective spillover effect approach," *Journal of Multinational Financial Management*, vol. 60, 2021.

[43] F. W. Xu, "Modeling the Paths of China's Systemic Financial Risk Contagion: A Ripple Network Perspective Analysis," *Computational economics*, vol. 63, 2022.

[44] F. Duarte and T. M. Eisenbach, "Fire-sale spillovers and systemic risk," *The Journal of Finance*, vol. 76, no. 3, pp. 1251–1294, 2021.

[45] J. Barunik, M. Bevilacqua, and R. Tunaru, "Asymmetric network connectedness of fears," *The Review of Economics and Statistics*, vol. 104, no. 6, pp. 1304–1316, 2022.

[46] T. Bollerslev, A. J. Patton, and R. Quaedvlieg, "Realized semibetas: disentangling "good: and "bad" downside risks," *Journal of Financial Economics*, vol. 144, no. 1, pp. 227–246, 2022.

[47] L. B. Feng and Y. L. Shi, "Markov regime-switching autoregessive model with tempered stable distribution: simulation evidence," *Studies in Nonlinear Dynamics & Econometrics*, vol. 24, no. 1, 2020.

[48] C. L. Weise, "The asymmetric effects of monetary policy: a nonlinear vector autoregression approach," *Journal of Money, Credit, and Banking*, vol. 31, no. 1, pp. 85–108, 1999.

[49] G. Caggiano, E. Castelnuovo, and J. M. Figueres, "Economic policy uncertainty spillovers in booms and busts," *Oxford Bulletin of Economics & Statistics*, vol. 82, no. 1, pp. 125–155, 2020.

[50] X. L. Gong, X. Xiong, and W. Zhang, "Research on systemic risk measurement and spillover effect of financial institutions in China," *Management World*, vol. 36, no. 08, pp. 65–83, 2020.

[51] G. J. Wang, Z. S. Xu, and C. Xie, "Connectedness and systemic risk contribution of Chinese financial institutions: a perspective from tail risk spillover network," *Journal of management sciences in China*, vol. 25, no. 5, pp. 109–126, 2022.

[52] Y. Chen, D. X. Mo, and Z. Z. Xu, "A study of interconnections and contagion among Chinese financial institutions using a Delta CoVaR network," *Finance Research Letters*, vol. 45, 2022.